Numerical study on laminar burning velocity and ignition delay time of ammonia flame with hydrogen addition

Jun Li [a], Hongyu Huang [b,c*], Noriyuki Kobayashi [a,*], Chenguang Wang [b,c], Haoran Yuan [b,c]

[a] *Department of Chemical Engineering, Nagoya University, Nagoya, Aichi 464-8603, Japan*

[b] *Guangzhou Institute of Energy Conversion, Chinese Academy of Sciences, Guangzhou 510640, China*

c Guangdong Key Laboratory of New and Renewable Energy Research and Development, Guangzhou 510640, China

Corresponding author

[*]Hongyu Huang, Tel.: +86 2037210762. Fax: +86 2087013240

E-mail address: huanghy@ms.giec.ac.cn

[*]Noriyuki Kobayashi, Tel.: +81 0527892733. Fax: +81 0527895428

E-mail address: kobayashi@energy.gr.jp

ABSTRACT

This study focuses on the application of NH_3 as a carbon-free alternative fuel in internal combustion devices. The two key parameters for fuel combustion, namely, laminar burning velocity and ignition delay time of the NH_3 flame at various H_2 blending levels, are numerically investigated. Results show that the selected modified Dagaut-Kéromnès mechanism is acceptable and repeatable for calculating the burning velocity and ignition delay time of NH_3-air flame at various H_2 addition conditions. H_2 addition increases the reactivity of NH_3 combustion at all conditions and enhances the burning velocity. This enhancement is mainly due to chemical effect caused by the reduction in chemical activation energy and the transport effect resulting from the high mobility of H_2. Furthermore, an increase in pressure and H_2 addition ratios can significantly decrease the ignition delay time of NH_3 mixtures and promote NH_3 ignition. The enhancement of H_2 addition on NH_3 ignition and laminar burning velocity is mainly attributed to the

contribution of the three following reactions: $O + H_2 = OH + H$, $H + O_2 = OH + O$, and $H_2 + OH = H_2O + H$. These reactions can significantly increase the concentration of free radicals and accelerate the peak of radicals.

Keywords: laminar burning velocity; ignition delay time; ammonia flame; hydrogen addition

1. Introduction

In recent decades, the study of alternative and clean fuels has attracted increasing attention with the depletion of fossil fuels and strengthening of pollutant emission regulations [1,2]. One of the prospective alternative fuels is NH_3 [3]. NH_3 is recognized as one of the most promising alternative fuels demonstrating the following favorable properties: (a) free of CO_2, SO_x, and soot emission because no carbon is present in this fuel [3–5]; (b) synthesized from fossil fuels (e.g., petroleum, coal, and natural gas), or renewable sources (such as wind, solar, hydropower, and biomass) [5–7]; and (c) easily and economically stored and transported in the liquid phase in large quantities via NH_3 tanks, trucks, ships and pipelines [5–7]. Therefore, NH_3 has become a key alternative fuel candidate. NH_3 has been utilized in specific energy devices, such as industry gas turbines and gas engines operated at high pressure and temperature [8,9].

As a fundamental property for fuel combustion in practical energy devices, laminar burning velocity is determined by the combined properties of diffusivity, exothermicity, and reactivity of a fuel. The laminar burning velocity is a key parameter to describe flame stabilization, extinction limits, flame structures, and velocity [10–12]. Unfortunately, the burning velocity of NH_3 is usually low around 5–13 cm/s [6,7,13]. This low value obstructs its application in specific energy devices. NH_3 combustion at various conditions, such as dual fuel with H_2 [7,14–18] and CH_4 [19–21]with high burning velocity, preheating condition [9,22, 23] from exhaust heat, and O_2-enriched condition [24,25], has been investigated to improve the laminar burning velocity of NH_3. Lee et al [16] investigated the burning velocity and emission characteristics of NH_3 with H_2 addition ratio from 0% to 50%. They found that the laminar burning velocity substantially increases with H_2 addition, and low NO_x formation occurs at fuel-rich conditions. Li et al. [17]

experimentally studied the combustion characteristics and NO_x formation of NH_3–H_2 combustion with H_2 ratio from 33.3 % to 60.0 %. The laminar burning velocity improved to a favorable level, similar to CH_4; whereas NO_x emission should be further treated when NH_3 is used as a fuel. The laminar burning velocities of pure NH_3 combustion at preheating and O_2-enriched conditions have also been studied by Li et al. [23,25]. Preheating temperature and O_2 enrichment positively affect the laminar burning velocity of NH_3 because of the high reaction rate and free radical formations. Furthermore, NO reacts with NH_x radicals and leads to low NO formation. Reducing NO emission in NH_3-air combustion is also observed.

Ignition delay time is another key property for fuel combustion in practical energy devices. It is a significant validation parameter in the development of chemical kinetics. The ignition delay time directly determines the ignition of fuel in practical energy devices. The fuel ignition process is recognized as zero-dimensional and homogeneous in a standard shock tube measurement facility. For NH_3 combustion, the ignition temperature and ignition energy of NH_3 are high and limit the application of NH_3 as a practical fuel. Therefore, the studies on the ignition characteristics of NH_3 and the enhancement of NH_3 ignition are necessary. Many studies [26–32] on application of NH_3 in compression-ignition and spark-ignition engines have been reported. However, previous experiments showed shortage with poor ignition property of NH_3. Additionally, little work has been conducted on the ignition delay time of NH_3 [33] and enhancement of NH_3 ignition. However, the fundamental key properties of NH_3, such as burning velocity, auto-ignition temperature, and minimum ignition energy are far apart with H_2, methanol, and gasoline as shown in Table 1 [30,31]. The burning velocity of NH_3 is only approximately 0.42% of H_2 (3.51 m/s), and the minimum ignition energy is 4440 times of H_2 (0.0018 mJ). By mixing with H_2, it is possible for NH_3 to present promising properties at suitable H_2 addition ratios. Furthermore, the kinetic of NH_3 combustion at various H_2 addition conditions remains also unclear and needs further investigation. Thus, studies on the laminar burning velocity and ignition delay time of NH_3 combustion are still rare and worthwhile.

This study are aims to evaluate the kinetic models of NH_3 combustion, investigate the laminar burning

velocity at various H_2 addition ratios (up to 90%), calculate the ignition delay time of NH_3 flames at various conditions, and discuss the effect of H_2 addition on the chain reaction mechanism, laminar burning velocity. The results will be used to provide a fundamental database and a favorable method for the enhancement of NH_3 combustion in practical energy devices.

2. Numerical simulations

The laminar burning velocity is simulated by a freely propagating adiabatic, premixed, laminar flame speed calculation model [34] in CHEMKIN 4.0. The hybrid time–integration/Newton-iteration technique with adaptive meshes and mixture–averaged transport parameters is applied to solve the steady–state mass, species and energy conservation equations of the flames; this technique has been described in detail in previous studies [22,23,25]. The inlet gas molar fractions for laminar burning velocity calculation at various H_2 addition ratios are summarized in Tables S1–S6 in Appendix A1. Estimated values for the initial, intermediate and production fractions along with temperature profiles are set before the simulations. The final solution is obtained at adaptive grid control based on the solution gradient and curvature (GRAD and CURV) set as 0.01 and 0.05, respectively. These values are sufficiently accurate for our results. The burning velocity is calculated with Soret effect using multicomponent transport method in CHEMKIN [34], which is shown as following equation based on Metghalchi and Kech power-low relation [25,35]:

$$S_u = S_{u0}\left(\frac{T_u}{T_0}\right)^{\alpha}\left(\frac{p}{p_0}\right)^{\beta}$$

where S_u is the laminar burning velocity (cm/s), T_u and p is the unburned temperature (K) and pressure (atm), S_{u0}, α, and β are constants, and the subscript 0 represents the standard state.

The ignition delay time is calculated using CHEMKIN package. A homogeneous charge compression-ignition model is selected for the simulations. A wide range of engine related conditions is investigated with pressure from 1.4 atm to 30 atm, temperature from 1500 K to 2500 K, and equivalence ratio from 0.5 to 2.0. The calculated ignition delay time of τ_{NH_2} and τ_{OH} is defined as the time interval between zero to the maximum molar fraction of NH_2, and OH radical. The ignition process is calculated by

constraining pressure and solving the energy equation. The end ignition time is set as 0.5s, which is quite enough for the ignition process. The initial temperature and pressure, along with the inlet gas composition, are set at the beginning of simulations. The inlet gas compositions for calculating the ignition delay time of NH_3 flames at various H_2 addition ratios are summarized in Table S7 in Appendix A2.

Three mechanisms are employed in this research, namely, modified Dagaut–Kéromnès (DK) mechanism [36,37], Millar–Bowman (MB) mechanism [38], and Reductive Konnov (RE) mechanism [39]. There are 43 species and 271 elementary reactions containing 40 elementary reactions for H_2/CO chemistry from Kéromnès [37] in the DK mechanism. The replacement of H_2/CO chemistry from Kéromnès is proved to improve the prediction for the ignition delay time and laminar burning velocity of NH3 for involving mixture with H_2 and O_2. The DK mechanism can simulate the oxidation of NH_3, H_2, and carbon monoxide at elevated temperature and pressure conditions. The MB mechanism is a C4 kinetic model (including 58 species and 255 elementary reactions) in which the NH_3 oxidation reaction developed by Sandia National Laboratories and Stanford University is considered, which has confirmed to be a significant mechanism for NH_3 oxidation process during hydrocarbon combustion. The RE mechanism is a NH_3/H_2 kinetic model with 19 species and 80 elementary reactions established by the Université Catholique de Louvain. The RE mechanism was developed from reduction of Konnov mechanism, those small quantities ($<10^{-8}$ mole fraction) and not necessary species for the formation and decomposition of main species are removed to obtain RE mechanism with only 19 species and 80 elementary reactions. These three mechanisms have been validated and added in Appendices B1–B3.

3. Results and discussion

3.1 Laminar burning velocity

Fig. 1 shows the burning velocity of NH_3-air flame at various H_2 addition ratios (X_{H_2}) and equivalence ratios of (a) 0.80, (b) 1.00, and (c) 1.25. The simulated results in this study by the DK and RE mechanisms are compared with the measured results by Lee et al. [16], Li et al. [17], Lindstedt [40],

Kumar [41], and Ichikawa [42], as well as the simulated results by Li et al. [22, 23] with the MB mechanism [38]. Fig. 1 shows that the simulated results are in good agreement with previous findings. Meanwhile, Li et al. [25] found that the calculated laminar burning velocity based on the RE mechanism is larger than measured results but consistent with the previously predicted values for NH_3-air flame. The laminar burning velocity of NH_3-air flame by the DK mechanism in this study shows better agreement with those measured results than the RE mechanism at all H_2 addition and equivalence ratio ranges. Particularly, at equivalence ratio of 1.00, the predicted burning velocity under DK mechanism match more closely with experimental data (within ~15%) than that of RE mechanism (10%~98%) under all H_2 addition conditions, same tendency is also observed at fuel lean and fuel rich conditions. Therefore, this agreement in burning velocity confirms that the selected DK mechanism is acceptable and repeatable for calculation of the burning velocity of NH_3-air flame at various H_2 addition conditions.

Fig. 2 shows the calculated laminar burning velocity of NH_3-air flame as a function of ϕ, with X_{H_2} as a parameter. The values of the laminar burning velocity of NH_3-air flame as a function of ϕ at various X_{H_2} are shown in Table S8 in Appendix C. The burning velocity of NH_3-air flame for X_{H_2} is used as the reference line. With increasing H_2 addition, thereby increasing X_{H_2}, the laminar burning velocity increases as expected. Previous studies suggested that the laminar burning velocity has linear correlations with certain key radicals [25]. The laminar burning velocity of hydrocarbon and hydrogen fuel is linearly correlated with H and OH radicals [25,43]. However, the laminar burning velocity of NH_3 is linearly correlated with NH_2 radical [25], which differs from that of hydrogen and hydrocarbon fuels. Therefore, the burning velocity of NH_3-air flame blending with H_2 can be correlated quasi-linearly with $(NH_2+H+OH)_{max}$, as shown in Fig. 3. This correlation is expressed as follows.

$$S_u = k * (NH_2 + H + OH)_{max} \ cm/s$$

where k is the slope, which represents the sensitivity of the laminar burning velocity of NH_3-air flame to the maximum mole fraction of (NH_2+H+OH) in the flame and equals 3758.5.

The laminar burning velocity of NH_3-air flame increases with the increase in X_{H_2}. H_2 addition with X_{H_2} = 0.3 shows a 192% increase in burning velocity (from 3.96 cm/s at pure NH_3 condition to 11.55 cm/s at X_{H_2} = 0.3) at ϕ of 0.8, whereas 169% (from 6.83 cm/s at pure NH_3 condition to 18.37 cm/s at X_{H_2} = 0.3) and 198% increases (from 6.62 cm/s at pure NH_3 condition to 19.71 cm/s at X_{H_2} = 0.3) are found at ϕ of 1.0 and 1.25, respectively. These effects can be considered as thermal because the increase in adiabatic flame temperature (as shown in Fig. 4), chemical because the reduction in chemical activation energy, and transport because of the high mobility of H_2. The thermal effect $\Delta S_{u,therm}$ and chemical effect $\Delta S_{u,chem}$ of H_2 addition on the laminar burning velocity can be defined as follows [44–46]:

$$\Delta S_{u,therm} = \frac{S_{u,T}(X_{H_2}) - S_u(X_{H_2} = 0)}{S_u(X_{H_2}) - S_u(X_{H_2} = 0)}$$

$$\Delta S_{u,chem} = \frac{S_{u,C}(X_{H_2}) - S_u(X_{H_2} = 0)}{S_u(X_{H_2}) - S_u(X_{H_2} = 0)}$$

Therefore, the transport effect of H_2 addition on the laminar burning velocity can be expressed as:

$$\Delta S_{u,tran} = 1 - \Delta S_{u,therm} - \Delta S_{u,chem}$$

where, $\Delta S_{u,therm}$, $\Delta S_{u,chem}$, and $\Delta S_{u,tran}$ are the thermal, chemical, and transport effects of H_2 addition on the laminar burning velocity respectively; $S_u(X_{H_2} = 0)$ is the laminar burning velocity of pure NH_3 as a modified baseline fuel mixture; $S_u(X_{H_2})$ is the laminar burning velocity of NH_3 at H_2 addition of X_{H_2}; $S_{u,T}(X_{H_2})$ is the laminar burning velocity of NH_3 at H_2 addition of X_{H_2} caused by the thermal effect, which is calculated by replacing part of nitrogen into argon to increase the baseline flame temperature; and $S_{u,C}(X_{H_2})$ is the laminar burning velocity of NH_3 at H_2 addition of X_{H_2} caused by the chemical effect, which is calculated by replacing part of nitrogen into CO_2 to decrease the H_2-added NH_3 flame temperature to the baseline flame temperature. The thermal, chemical, and transport effects of H_2 addition on the laminar burning velocity of NH_3-air flame at various X_{H_2} are shown in Fig. 5. The thermal, chemical, and transport effects of H_2 addition all contribute to the enhancement in the laminar burning velocity. The laminar burning velocity enhancement of NH_3-air flame caused by the chemical and transport

effects is about 10 times of that by the thermal effect. Furthermore, at low H_2 addition ratios, the chemical effect plays a dominant role. The transport effect increases with rising H_2 addition ratios. Both the chemical and transport effects are the main reasons for the burning velocity enhancement at high H_2 addition ratios. High reactivity and mobility of H_2 lead to high chemical and transport effects. Similar results are obtained at fuel-lean (ϕ of 0.8) and fuel-rich conditions (ϕ of 1.25).

Results of sensitivity analysis of key elementary reactions that contribute to the enhancement of the laminar burning velocity of NH_3-air flame at various H_2 addition ratios are shown in Fig. 6. The sensitivities of elementary reactions of R235: $O + H_2 = OH + H$ and R239: $H_2 + OH = H_2O + H$ increase significantly with H_2 addition ratios. The most important elementary reaction of H_2 addition on laminar burning velocity of NH_3-air flame is R236: $H + O_2 = OH + O$. The sensitivity coefficient of R236 is non-monotonically changed with X_{H_2}, whereas, the sensitivity of R235: $O + H_2 = OH + H$, and R239: $H_2 + OH = H_2O + H$ on the laminar burning velocity of NH_3-air flame emerges at X_{H_2} of 0.3 and increases with increasing X_{H_2}. The acceleration of R235, R236, and R239 with H_2 addition can enhance H, O, and OH radicals, which are crucial to the NH_3 decomposition reaction. The following three reactions are necessary to form NH_2 radical:

$$NH_3 + OH = NH_2 + H_2O \quad \text{(R93)}$$

$$NH_3 + H = NH_2 + H_2 \quad \text{(R91)}$$

$$NH_3 + O = NH_2 + OH \quad \text{(R92)}$$

The enhancement of NH_3 decomposition is directly related to the burning velocity improvement of NH_3. According to previous discussions on NH_3 combustion at preheating and O_2-enriched conditions, the enhancement of H abstraction of NH_3 attacked by O, H, OH, and M radicals is caused by thermal decomposition reactions, which can also be proven to increase the burning velocity of NH_3 flame [22,23,25]. Therefore, R235: $O + H_2 = OH + H$, R236: $H + O_2 = OH + O$, and R239: $H_2 + OH = H_2O + H$ are most sensitive reactions on the burning velocity of NH_3-air flame with H_2 addition.

3.2 Ignition delay time

3.2.1 Ignition delay time validation

As a key parameter of fuel combustion in energy devices, the ignition delay time of NH_3 flame during the NH_3 auto-ignition process in a closed homogeneous batch reactor at various X_{H_2} conditions is calculated. Figs. 7(a)–7(c) show comparisons between the experimental data [33] and numerical results of the ignition delay time based on NH_2 and OH radical using the DK, MB, and RE mechanisms at equivalence ratios of 0.5, 1.0, and 2.0, respectively. Fig. 7 shows that the predicted ignition delay of the NH_3-O_2 mixture for each mechanism differs over all temperature and equivalence ratio ranges and has a maximum difference of up to one order of magnitude. Among these mechanisms, the ignition delay time of the DK mechanism based on NH_2 radical can be predicted well with the experimental data by Mathieu and Petersen [33] compared with that of the MB and RE mechanisms. Particularly, at equivalence ratio of 1.00, the predicted ignition delay time (τ_{NH_2}) under DK mechanism match more closely with experimental data (within ~14%) than that at RE mechanism (approximately 40%~70%) under all H_2 addition conditions, same tendency is also observed equivalence ratios of 0.5 and 2.0. Therefore, the DK mechanism is selected for the following ignition delay discussion. The specific selection of the DK mechanism does not alter the generality of the discussion. In other words, the main and controlling reactions for NH_3 ignition are the same, whereas the kinetic parameters are different from other mechanisms.

For the fuel-lean and stoichiometric conditions as shown in Fig. 7(a) and 7(b), the simulated results agree well with the experimental data [33]. For the fuel-rich condition shown in Fig. 7(c), the simulated results are one or two times larger than the experimental data [33]. Although the selected kinetic mechanism can predict the laminar burning velocity and ignition delay time for almost all operating conditions, its ability to predict the ignition delay time for NH_3 combustion is less reliable at fuel-rich conditions.

3.2.2 Ignition delay time at various hydrogen addition

Fig. 8(a)–8(c) show the effect of H_2 addition on the ignition delay time for the NH_3-O_2 mixture diluted in 99% at various ϕ of 0.5, 1.0, and 2.0 respectively. The ignition delay time of NH_3 is dramatically reduced with H_2 addition over all tested conditions. In particular, at a high temperature (1950 K), the reduction in ignition delay time is 93.2% at ϕ of 0.5 and increases to 93.6% and 93.7% at ϕ of 1.0 and 2.0, respectively. Meanwhile, H_2 addition shows a strong effect on activation energy (E_a) changes (50.3 kcal mol^{-1} for X_{H_2} = 0, and 17.9 kcal mol^{-1} for X_{H_2} = 0.9 at ϕ of 1.0 and pressure of 1.4 atm) as shown in Table 1.

Fig. 9 shows the effect of pressure on the ignition delay time for NH_3-O_2-Ar mixture at various X_{H_2}. The black, red, and blue lines show the simulation results, whereas the dots are the measurement results of NH_3-O_2-Ar mixture by Mathieu and Petersen [33] at 1.4, 11, and 30 atm. Fig. 9 shows that an increase in pressure can significantly decrease the ignition delay time of NH_3 mixtures and promote of NH_3 ignition. The addition of H_2 does not change the pressure dependence phenomenon of the NH_3 ignition delay time. Interestingly, the reduction in the ignition delay time with pressure changing from 1.4 atm to 10 atm is more pronounced than that from 10 atm to 30 atm. The reaction rate of the two most significant dominant radicals during NH_3 ignition process (i.e., OH reaction together with elementary reactions of R92: $NH_3 + O = NH_2 + OH$, R235: $O + H_2 = OH + H$, and R236: $H + O_2 = OH + O$ for OH radical production, as well as NH_2 reaction together with elementary reactions of R93: $NH_3 + OH = NH_2 + H_2O$, R91: $NH_3 + H = NH_2 + H_2$, and R92: $NH_3 + O = NH_2 + OH$ for NH_2 production) increases with increasing pressure and H_2 addition ratios (Fig. 10). The enhancement of OH radical can increase unreactive species of NH_3 into reactive NH_2, NH, and N radicals with H abstraction of NH_3 decomposition. Furthermore, the enhancement in the reaction rate of OH radical from 10 atm to 30 atm is much higher than that from 1.4 atm to 10 atm. This difference leads to a more significant reduction in the ignition delay time. The solid black lines in Fig. 9 shows that the ignition delay time of pure NH_3 decreases with increasing pressure at ϕ ranging from 0.5 to 2.0. The effect of ϕ on the ignition delay time for NH_3-O_2-Ar mixture at various H_2 addition ratios and pressure of 1.4 atm is shown in Fig. 11. The solid, dash, and dot lines are the simulation

results at H_2 addition ratios of 0.0%, 50.0%, and 90%, respectively. For pure NH_3 mixture, only a minimal effect is observed when ϕ increases from 0.5 to 2.0. At high X_{H_2}, the effect becomes obvious with a change in ϕ. This finding indicates that NH_3 ignition has a strong X_{H_2} dependence upon ϕ.

NH_3 ignition is closely related to the H_2 addition ratio, pressure, and equivalence ratio. To quantitatively understand the pressure-dependent behavior in NH_3 ignition, the effect of pressure on the reduction ratio of the ignition delay time at 1950 K and various ϕ of 0.5, 1.0, and 2.0 is shown in Fig. 12(a)–12(c), respectively. Fig. 12 shows that the reduction ratio of the ignition delay time increases with an increase in H_2 addition ratio but decreases with rising pressure at all equivalence ratios. At fuel-lean and stoichiometric conditions, the reduction at high pressure is similar to that at low pressure and shows small pressure-dependent effects. For fuel-rich conditions, the pressure-dependent effects on the ignition delay time become large. To quantitatively understand the equivalence ratio-dependent behavior in NH_3 ignition, the effects of the equivalence ratio on the reduction ratio of the ignition delay time at 1950 K and various pressures of 1.4, 11, and 30 atm is shown in Figs. 13(a)–13(c), respectively. As shown in Fig. 13, the reduction of ignition delay time increase with increasing H_2 addition ration at all equivalence ratio. At lower pressure below 11.0 atm, equivalence ratio effect on the reduction ratio of ignition delay time is similar. Specifically, at same pressure of 11 atm and H_2 addition ration of 0.3, the reduction ratio of ignition delay time reaches 78.6%, 75.7%, and 76.9% at stoichiometric condition, fuel-lean and fuel rich conditions, respectively. At high pressure of 30.0 atm, H_2 addition provides the strongest effect on the reduction ratio of ignition delay time at stoichiometric condition. The reduction ratio of ignition delay time at stoichiometric condition reaches 78.2%, which is about 5% higher than that at fuel-lean (74.2%) and fuel rich (74.7%) conditions at H_2 addition ration of 0.3. However, the reduction at fuel-lean and fuel-rich conditions exhibits similar increasing tendency on NH_3 ignition with H_2 addition.

3.2.3 Sensitivity analysis

To further identify the important reactions for NH_3 ignition, sensitivity analysis on the OH radical is

performed at various H_2 addition ratios and pressures. Previous studies showed that sensitivity analysis of OH and NH_2 produces results that are crucial to NH_3 oxidation and combustion [25,33]. Furthermore, the formation of OH free radical is closely related to NH_3 decomposition. Therefore, OH sensitivity analysis is highly similar to sensitivity analysis of the ignition delay time. The dominant reactions from OH radical sensitivity analysis can be assumed as the important reactions for NH_3 ignition.

Fig. 14 shows the results of normalized sensitivity analysis at certain selected conditions. For fuel-lean condition, Figs. 14(a)–14(c) illustrate the results at ϕ = 0.5, 1950 K, and pressure of 1.4, 11, and 30 atm at X_{H_2} of 0.0, 0.5, and 0.9, respectively. The two most enhancing reactions are R235: O + H_2 = OH + H, and R236: H + O_2 = OH + O, and the most inhibiting reaction is R239: H_2 + OH = H_2O + H. These reactions are revealed in sensitivity analysis. Apart from the three most effective reactions, R93: NH_3 + OH = NH_2 + H_2O, and R98: NH_2 + OH = NH + H_2O also show important effect on NH_3 ignition at H_2 addition and high pressure conditions.

At stoichiometric conditions, Figs. 14(d)–14(f) show the results at ϕ = 1.0, 1950 K, and pressure of 1.4, 11, and 30 atm at X_{H_2} of 0.0, 0.5, and 0.9, respectively. Sensitivity analysis at stoichiometric conditions shows that almost all important reactions are the same or nearly at the same order in terms of normalized sensitivity at fuel-lean conditions. The two most enhancing reactions are R235: O + H_2 = OH + H, and R236: H + O_2 = OH + O, whereas the most inhibiting reaction is R239: H_2 + OH = H_2O + H. These reactions are similar to the results of sensitivity analysis on burning velocity.

For fuel-rich condition, Figs. 14(g)–14(i) show the results at ϕ = 2.0, 1950 K, and pressure of 1.4, 11, and 30 atm at X_{H_2} of 0.0, 0.5, and 0.9, respectively. The reactions of R235: O + H_2 = OH + H, R236: H + O_2 = OH + O, and R239: H_2 + OH = H_2O + H are the also most important ones based on the results of sensitivity analysis. These reactions can significantly increase the concentration of free radicals and accelerate the peak of H, O, and OH; such events promote NH_3 ignition. The results of this sensitivity analysis show that the most inhibiting reaction of R239: H_2 + OH = H_2O + H becomes less important,

whereas R93: $NH_3 + OH = NH_2 + H_2O$ becomes dominant; this reaction is the thermal decomposition reaction of NH_3 (i.e., with involvement of NH_3 and OH radical). The importance of R93: $NH_3 + OH = NH_2 + H_2O$ illustrates some potential advantages at fuel-rich conditions, NH_3 can be completely consumed and converted to H_2, which has also been proved by previous studies [9,25,39].

4. Conclusions

This study focuses on the application of NH_3 as a carbon-free alternative fuel in internal combustion devices. The laminar burning velocity and ignition delay time of NH_3 flames at various H_2 blending levels have been numerically investigated. The main conclusions are summarized as follows:

(1) The addition of H_2 from thermal decomposition of NH_3 increases the reactivity of NH_3 combustion and enhances the burning velocity of NH_3, enabling NH_3 as a practical fuel in various energy devices.

(2) The enhancement of burning velocity of NH_3 is mainly due to the chemical effect caused by the reduction in chemical activation energy and transport effect resulting from the high mobility of H_2.

(3) An increase in pressure and H_2 addition ratios can significantly decrease the ignition delay time of NH_3 mixtures and promote of NH_3 ignition.

(4) The enhancement of H_2 addition on NH_3 ignition and laminar burning velocity is mainly attributed to the three following reactions: $O + H_2 = OH + H$, $H + O_2 = OH + O$, and $H_2 + OH = H_2O + H$. These reactions can significantly increase the concentration of free radicals and accelerate the peak of H, O, and OH radicals.

References

[1] Riaz A, Zahedi G, Klemeš JJ. A review of cleaner production methods for the manufacture of methanol. J Cleaner Product 2013;57: 19–37.

[2] Astbury GR. A review of the properties and hazards of some alternative fuels. Process Saf Environ 2008;86: 397–414.

[3] Zamfirescu C, Dincer I. Using ammonia as a sustainable fuel. J Power Sources 2008;185: 459–465.

[4] Zhao BT, Su YX, Cui GM. Post-combustion CO_2 capture with ammonia by vortex flow-based multistage spraying: Process intensification and performance characteristics. Energy 2016;102: 106–117.

[5] Um DH, Kim TY, Kwon OC. Power and hydrogen production from ammonia in a micro-thermophotovoltaic device integrated with a micro-reformer. Energy 2014;73: 531–542.

[6] Um DH, Joo JM, Lee S, Kwon OC. Combustion stability limits and NO_x emissions of nonpremixed ammonia-substituted hydrogen-air flames. Int J Hydrogen Energy 2013;38: 14854–14865.

[7] Wang FC, Zhou ZJ, Dai ZH, Gong X, Yu GS, Liu HF, Wang YF, Yu ZH. Development and demonstration plant operation of an opposed multi-burner coal-water slurry gasification technology. Front Energy Power Eng China 2007;1: 251–258.

[8] Verkamp FJ, Hardin MC, Williams JR. Ammonia combustion properties and performance in gas-turbine burners. Symp (Int) Combust 1967;11: 985–992.

[9] Duynslaegher C, Jeanmart H, Vandooren J. Ammonia combustion at elevated pressure and temperature conditions. Fuel 2010;89: 3540–3545.

[10] Aung KT, Hassan MI, Faeth GM. Flame stretch interactions of laminar premixed hydrogen/air flames at normal temperature and pressure. Combust Flame 1997;109: 1–24.

[11] Hu EJ, Li XT, Meng X, Chen YZ, Cheng Y, Xie YL, Huang ZH. Laminar flame speeds and ignition delay times of methane-air mixtures at elevated temperatures and pressures. Fuel 2015;158: 1–10.

[12] Bayraktar H, Durgun O. Investigation the effects of LPG on spark ignition engine combustion and performance. Energy Convers Manage 2005;46: 2317–2333.

[13] Ronney PD. Effect of chemistry and transport properties on near limit flames at microgravity. Combust Sci Technol 1988;59: 123–141.

[14] Kumar P. An experimental and numerical study of NO_x formation mechanisms in NH_3-H_2-Air flam. Iowa State University, 2012.

[15] Joo JM, Lee S, Kwon OC. Effects of ammonia substitution on combustion stability limits and NO_x emissions of premixed hydrogen-air flames. Int J Hydrogen Energy 2012;37: 6933–6941.

[16] Lee JH, Kim JH, Park JH, Kwon OC. Study on properties of laminar premixed hydrogen-added ammonia/air flames for hydrogen production. Int J Hydrogen Energy 2010;35: 1054–1064.

[17] Li J, Huang HY, Kobayashi NY, He ZH, Nagai YH. Study on using hydrogen and ammonia as fuels: combustion characteristics and NO_x formation. Int J Energ Res 2014;38: 1214–1223.

[18] Armjtage JW, Gray P. Flame speeds and flammability limits in the combustion of ammonia: ternary mixtures with hydrogen, nitric oxide, nitrous oxide or oxygen. Combust Flame 1965;9:173–184.

[19] Henshaw PF, D'andrea T, Mann KRC, Ting DSK. Premixed ammonia-methane-air combustion. Combust Sci Technol 2005;177:2151–2170.

[20] Pfahl U J, Ross M C, Shepherd J E, Pasamehmetoglu K O, Unal C. Flammability limits, ignition energy, and flame speeds in H_2-CH_4-NH_3-N_2O-O_2-N_2 mixtures. Combust Flame 2000;123: 140–158.

[21] Tian ZY, Li YY, Zhang LD, Glarborg P, Qi F. An experimental and kinetic modeling study of premixed NH_3/CH_4/O_2/Ar flames at low pressure. Combust Flame 2009;156: 1413–1426.

[22] Li J, Huang HY, Yuan HR, Zeng T, Yagami MY, Kobayashi NY. Modeling of ammonia combustion characteristics at preheating combustion: NO formation analysis. Int J Global Warming 2016;10: 230–241.

[23] Li J, Huang HY, Kobayashi NY, He ZH, Zeng T. Research on combustion and emission characteristics of ammonia under preheating conditions. J Chem Eng Jpn 2016; 49: 641–648.

[24] Takeishi H, Hayashi J, Kono S, Iino K, Akamatsu F. Characteristics of ammonia/N_2/O_2 laminar premixed flame in oxygen-enriched condition. 11th Annual NH_3 Fuel Conference 2014.

[25] Li J, Huang HY, Kobayashi NY, He ZH, Zeng T. Numerical study on effect of oxygen content in combustion air on ammonia combustion. Energy 2015;92: 2053–2068.

[26] Aaron JR, Song CK. Combustion and emissions characteristics of compression-ignition engine using dual ammonia-diesel fuel. Fuel 2011;90: 87–89.

[27] Boretti AA. Novel heavy duty engine concept for operation dual fuel H_2-NH_3. Int J Hydrogen Energy 2012;37: 7869–7876.

[28] Grannell SM, Assanis DN, Bohac SV, Gillespie DE. The fuel mix limits and efficiency of a stoichiometric, ammonia, and gasoline dual fueled spark ignition engine. J Eng Gas Turbines Power 2008;130: 1–8.

[29] Ryu K, Zacharakis-Jutz GE, Kong SC. Effects of gaseous ammonia direct injection on performance characteristics of a spark-ignition engine. Appl Energy 2014;116: 206–215.

[30] MØrch CS, Bjerre AMP, GØttrup SCS, Schramm J. Ammonia/hydrogen mixtures in an SI-engine: Engine performance and analysis of a proposed fuel system. Fuel 2011;90: 854–864.

[31] Liu R., Ting DSK, Checkel D. Ammonia as a fuel for SI engine. SAE Technical Paper 2003;01-3095: 1–7.

[32] Christopher WG, Song CK. Performance characteristics of a compression–ignition engine using direct – injection ammonia – DME mixtures. Fuel 2013;103: 1069–1079.

[33] Mathieu O, Petersen EL. Experimental and modeling study on the high-temperature oxidation of ammonia and related NO_x chemistry. Combust Flame 2015;162: 554–570.

[34] Miller JA, Smooke MD, Green RM, Kee RJ. Kinetic modeling of the oxidation of ammonia in flames. Combust Sci Technol 1983;34: 149–176.

[35] Metghalchi M, Keck J C. Burning velocities of mixtures of air with methanol, isooctane, and indolene at high pressure and temperature. Combust Flame 1982;48: 191–210.

[36] Dagaut P, Nicolle A. Experimental and kinetic modeling study of the effect of SO_2 on the reduction of NO by ammonia. Proc Combust Inst 2005;30: 1121–1218.

[37] Kéromnès A, Metcalfe WK, Heufer KA, Donohoe N, Das AK et al. An experimental and detailed chemical kinetic modeling study of hydrogen and syngas mixture oxidation at elevated pressures. Combust Flame 2013;160: 995–1011.

[38] Miller JA, Bowman CT. Mechanism and modeling of nitrogen chemistry in combustion. Prog Energ Combust Sci 1989;15: 287–338.

[39] Duynslaegher C, Jeanmart H, Vandooren J. Flame structure studies of premixed ammonia/hydrogen/oxygen/argon flames: Experimental and numerical investigation. Proc Combust Inst 2009;32: 1277–1284.

[40] Lindstedt RP, Lockwood FC, Selim MA. Detailed kinetic modeling of chemistry and temperature effects on ammonia oxidation. Combust Sci Tech 1994;99: 253–276.

[41] Kumar P, Meyer TR. Experimental and modeling study of chemical-kinetics mechanisms for H_2-NH_3-air mixtures in laminar premixed jet flames. Fuel 2013;108:166–76.

[42] Ichikawa AN, Hayakawa AH, Kitagawa YC, Somarathne KDKA, Kudo T, Kobayashi HA. Laminar burning velocity and Markstein length of ammonia/hydrogen/air premixed flames at elevated pressures. Int. J. Hydrogen Energy 2015;40:9570–78.

[43] Zhang W, Chen ZH, Shen YG, Shu GQ, Chen GS, Xu B, et al. Influence of water emulsified diesel & oxygen-enriched air on diesel engine NO smoke emissions and combustion characteristics. Energy 2013;55:369–77.

[44] Wang H, Hahn TO, Sung CJ, Law CK. Detailed oxidation kinetics and flame inhibition effects of chloromethane. Combust Flame 1996;105:291–307.

[45] Li ZS, Han W, Liu D, Chen Z. Laminar flame propagation and ignition properties of premixed iso-octane/air with hydrogen addition. Fuel 2015;158:443–450.

[46] Sung CJ, Huang Y, Eng JA. Effects of reformer gas addition on the laminar flame speeds and flammability limits of n-butane and iso-butane flames. Combust Flame 2001;126:1699–713.

Nomenclature

ϕ	Equivalence ratio (-)
X_{H_2}	H_2 addition ratio in NH_3 (-)
P	Pressure (atm)
T	Temperature (K)
S_u	Laminar burning velocity (cm s^{-1})
$\Delta S_{u,therm}$	Thermal effect on laminar burning velocity (-)
$\Delta S_{u,chem}$	Chemical effect on laminar burning velocity (-)
$\Delta S_{u,tran}$	Transport effect on laminar burning velocity (-)
$S_u(X_{H_2} = 0)$	Laminar burning velocity of NH_3 at H_2 addition ratio of 0 (cm s^{-1})
$S_u(X_{H_2})$	Laminar burning velocity of NH_3 at H_2 addition ratio of X_{H_2} (cm s^{-1})
$S_{u,T}(X_{H_2})$	Laminar burning velocity of NH_3 at H_2 addition of X_{H_2} caused by thermal effect (cm s^{-1})
$S_{u,C}(X_{H_2})$	Laminar burning velocity of NH_3 at H_2 addition of X_{H_2} caused by chemical effect (cm s^{-1})
τ_{NH_2}	Ignition delay time based on maximum molar fraction of NH_2 (μs)
τ_{OH}	Ignition delay time based on maximum molar fraction of OH (μs)
E_a	Activation energy (kcal mol^{-1})

Table 1.

Fundamental key properties of various fuels [30,31]

Items	Ammonia	Hydrogen	Methanol	Gasoline
Lower heating value / MJ/kg	18.8	120.1	19.7	44.5
Lower heating value / MJ/L	11.3	8.5	15.5	29.7
Laminar burning velocity / m/s	0.015	3.51	0.50	0.58
Flammability limits, gas in air / vol.%	15-28	4.7-75	6-36	0.6-8
Auto-ignition temperature / °C	651	571	470	230
Minimum ignition energy / mJ	8.0	0.0018	0.14	0.14
Density, 25°C, 1 atm / g/L	0.703	0.082	787	740

Table 2.

Activation Energy of NH_3-O_2-Ar mixtures at various H_2 addition ratio and pressure of 1.4 atm / kcal mol^{-1}

	X_{H2} / -						
	0.0		0.1	0.3	0.5	0.7	0.9
ϕ	Experimental data [33]	This work					
0.5	44.6	43.9	36.7	26.7	23.1	19.1	16.8
1.0	51.7	50.3	40.8	30.7	23.7	19.9	17.9
2.0	56.3	55.1	44.7	31.1	26.2	22.7	18.9

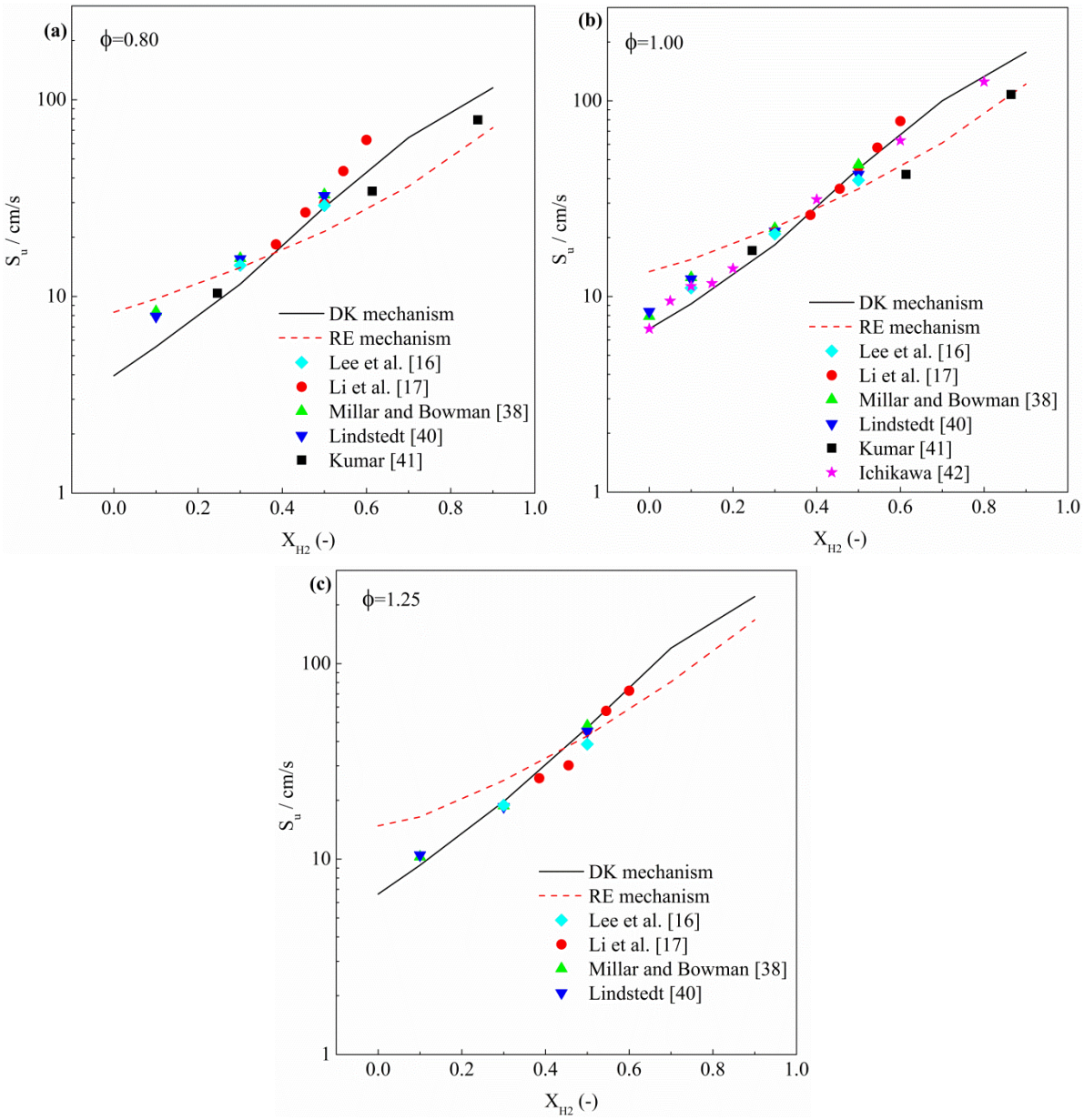

Fig. 1. Laminar burning velocity as a function of X_{H_2} at various equivalence ratios: (a) ϕ=0.80; (b) ϕ=1.00; (c) ϕ=1.25. Symbols: Measurements results by Lee et al. [16], Li et al. [17], Millar and Bowman [38], Lindstedt [40], Kumar [41], Ichikawa [42]; Line: Simulated results in this study.

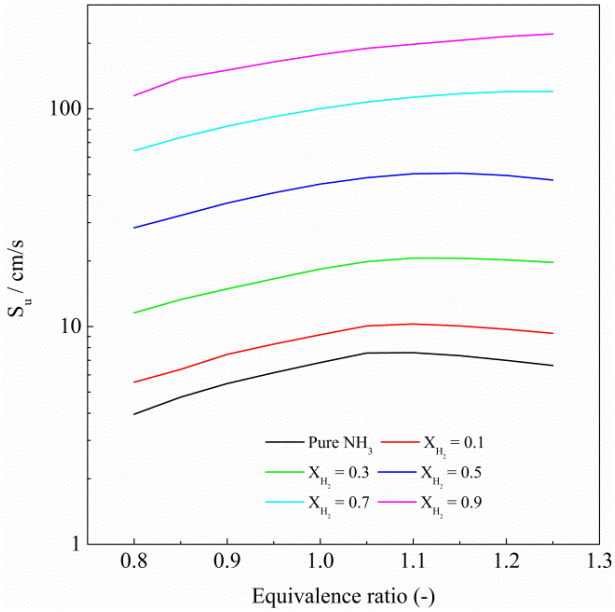

Fig. 2. The function of NH_3-air laminar burning velocity with equivalence ratios at various X_{H_2}.

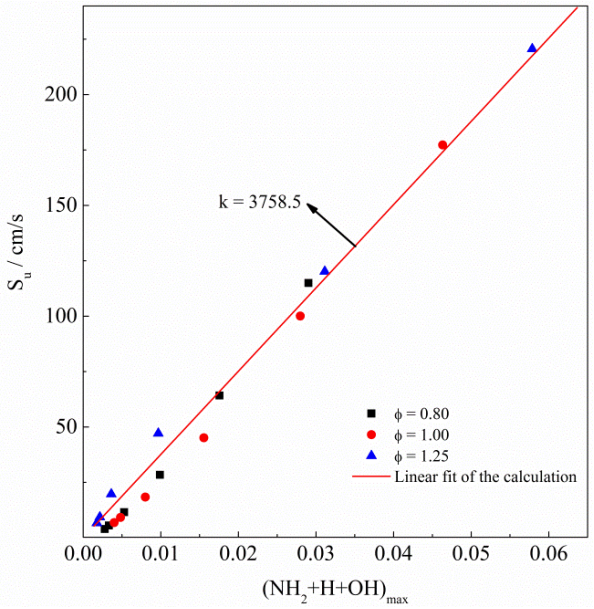

Fig. 3. Laminar burning velocity correlation with maximum mole fraction of NH_2+H+OH radicals.

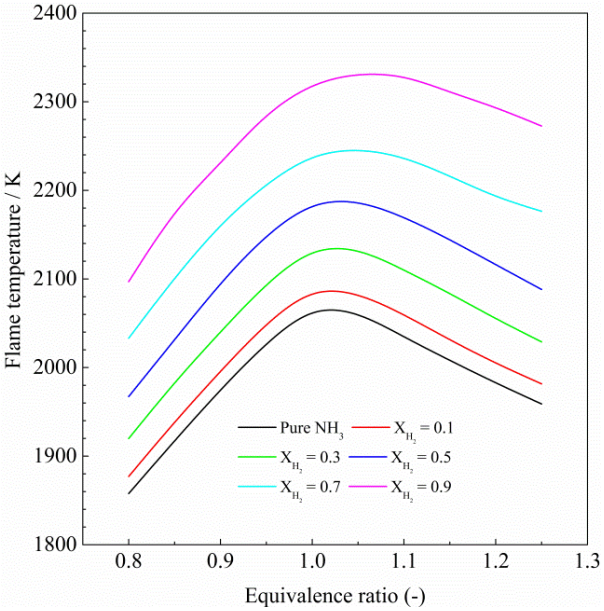

Fig. 4. The function of adiabatic flame temperature of NH_3-air flame with equivalence ratios at various X_{H_2}.

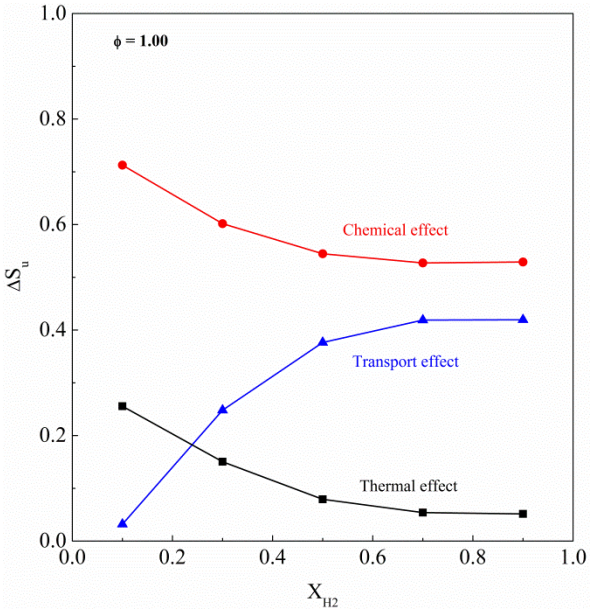

Fig. 5. Thermal, chemical, and transport effect of H_2 addition on the laminar burning velocity of NH_3-air flame (ϕ=1.0).

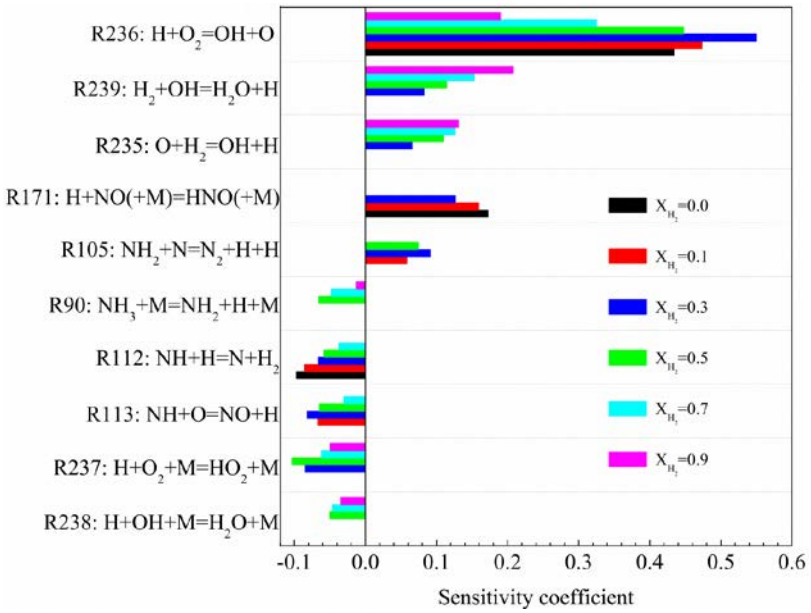

Fig. 6. The sensentivitiy analysis of elementary reactions to laminar burning velocity of NH_3-air flame at various X_{H_2} (ϕ=1.0).

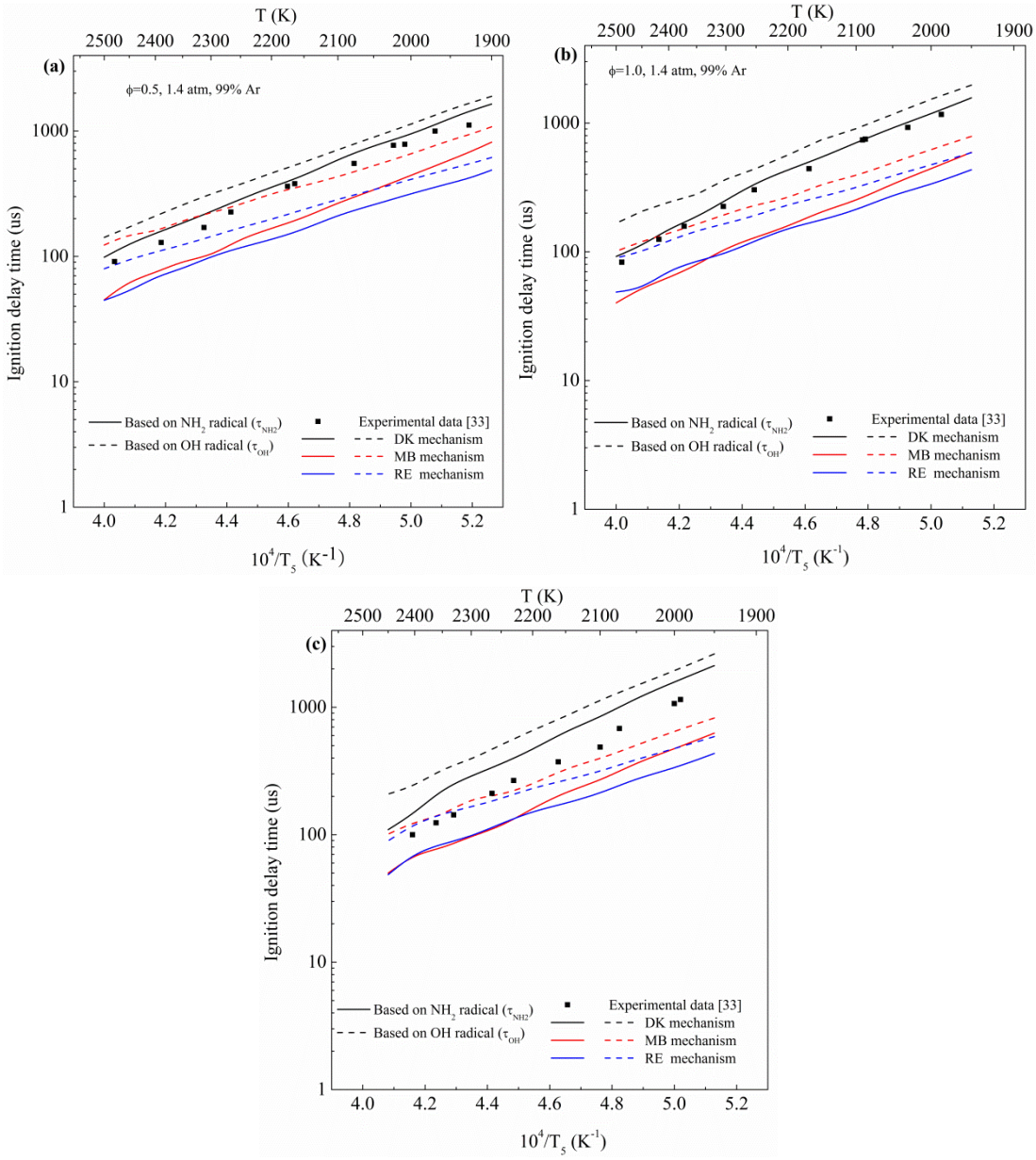

Fig. 7. Comparison between experimental and numerical ignition delay times based on NH_2 radical (Solid line) and OH radical (Dash line) for NH_3-O_2 mixture diluted in 99% Ar at various equivalence ratios: (a) ϕ=0.5; (b) ϕ=1.0; (c) ϕ=2.0.

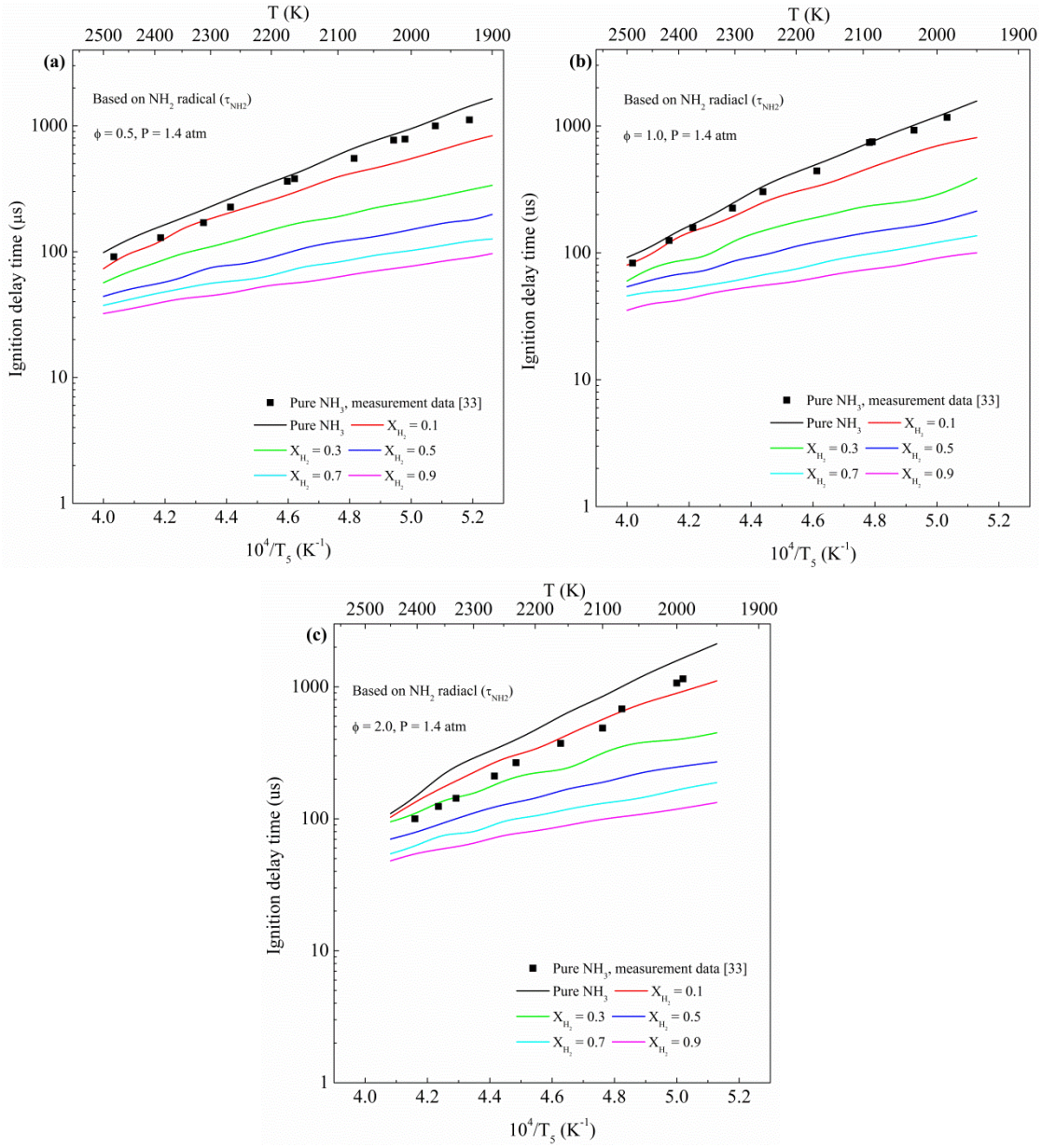

Fig. 8. Effect of H_2 addition on ignition delay times for NH_3-O_2 mixture diluted in 99% Ar at various equivalence ratios: (a) ϕ=0.5; (b) ϕ=1.0; (c) ϕ=2.0.

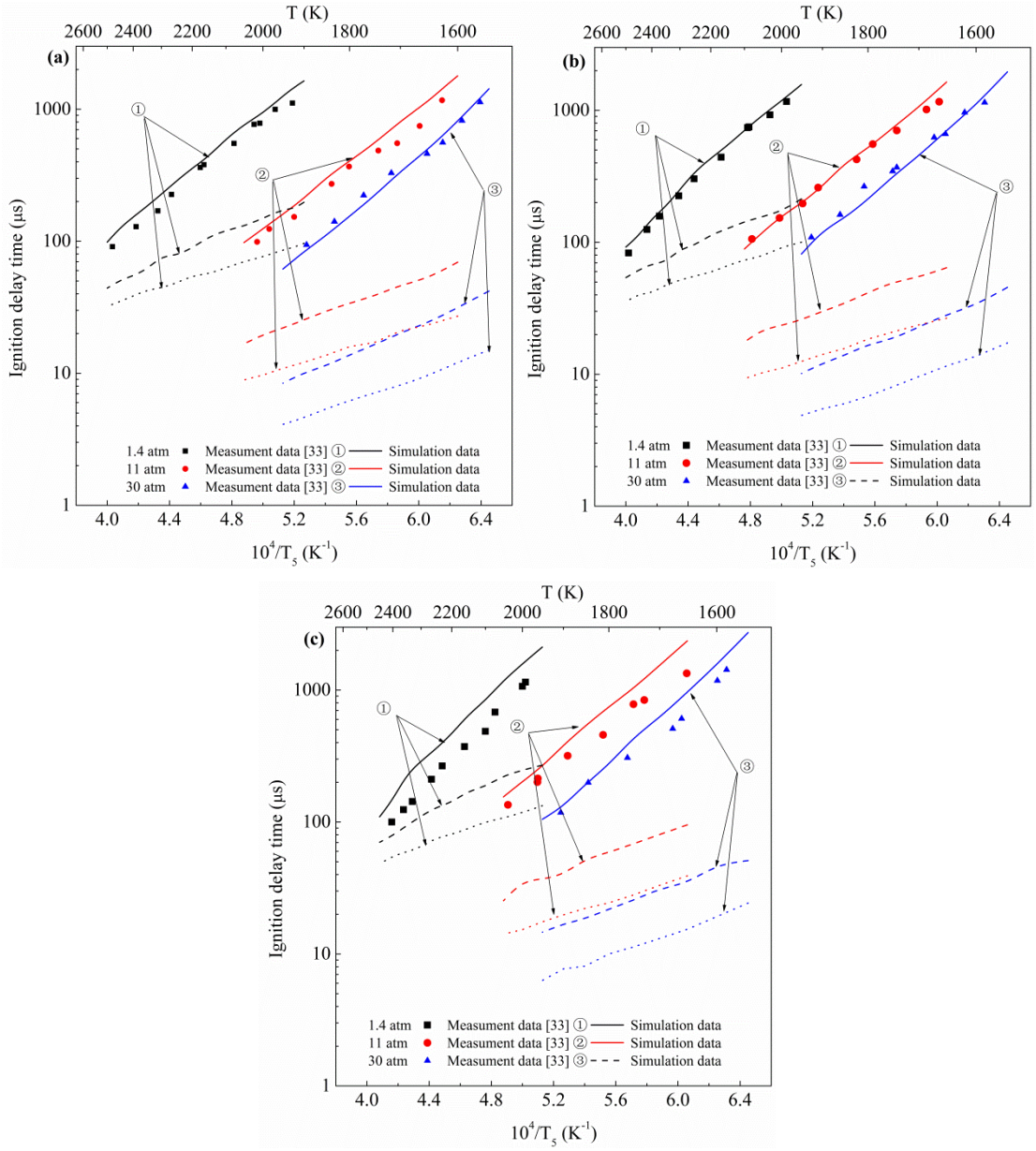

Fig. 9. Effect of pressure on ignition delay times for NH_3-O_2 mixture at H_2 addition ratio of 0 (Solid line), 0.5 (Dash line), and 0.9 (Dot line): (a) ϕ=0.5; (b) ϕ=1.0; (c) ϕ=2.0.

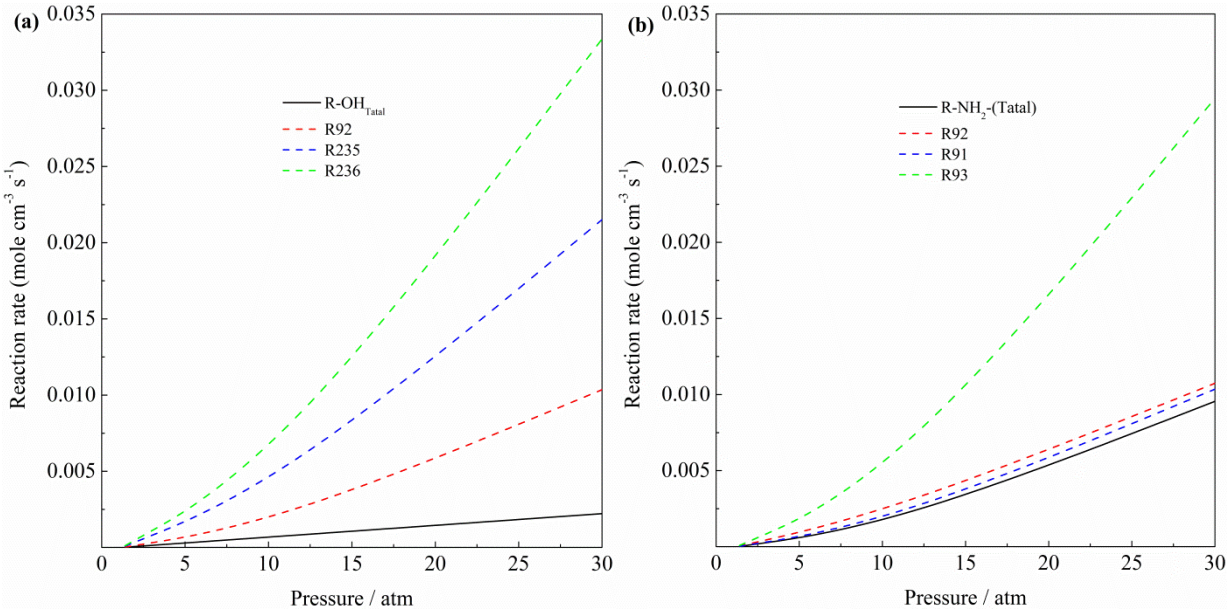

Fig. 10. Effect of pressure on total and elementary reaction rate of OH (a) and NH_2 (b) radicals at X_{H_2} of 0.5.

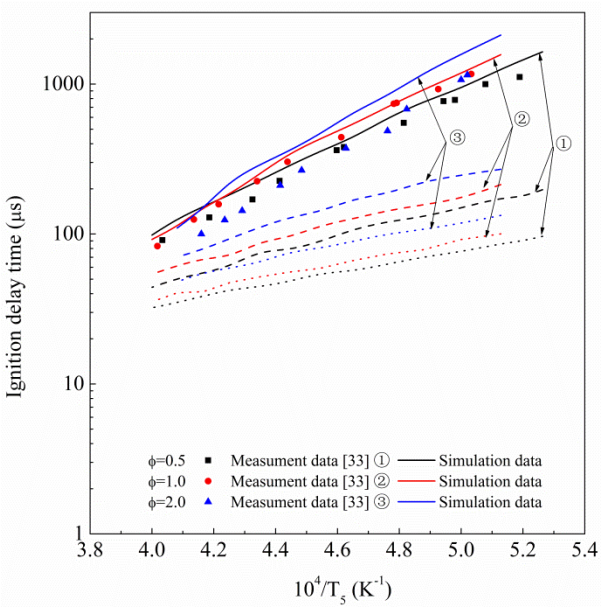

Fig. 11 Effect of ϕ on ignition delay time for NH_3-O_2-Ar mixture at pressure of 1.4 atm and various H_2 addition ratios of 0.0 (Solid line), 0.5 (Dash line), and 0.9 (Dot line).

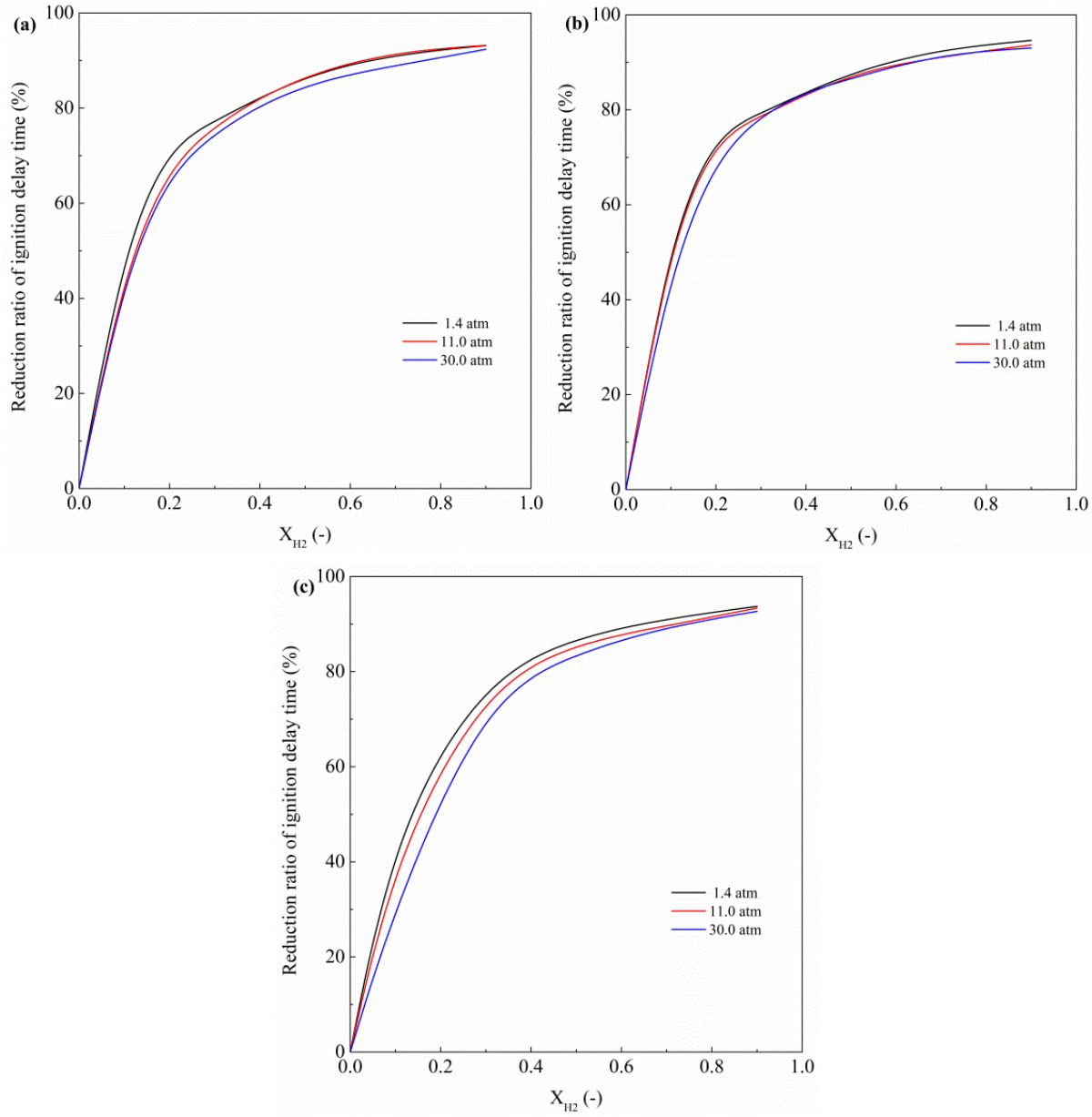

Fig. 12 Pressure effect on the reduction ratio of ignition delay time compared to pure NH_3 with various H_2 addition ratios over pressure of 1.4-30 atm at 1950 K: (a) ϕ = 0.50, (b) ϕ = 1.00, (c) ϕ = 2.0.

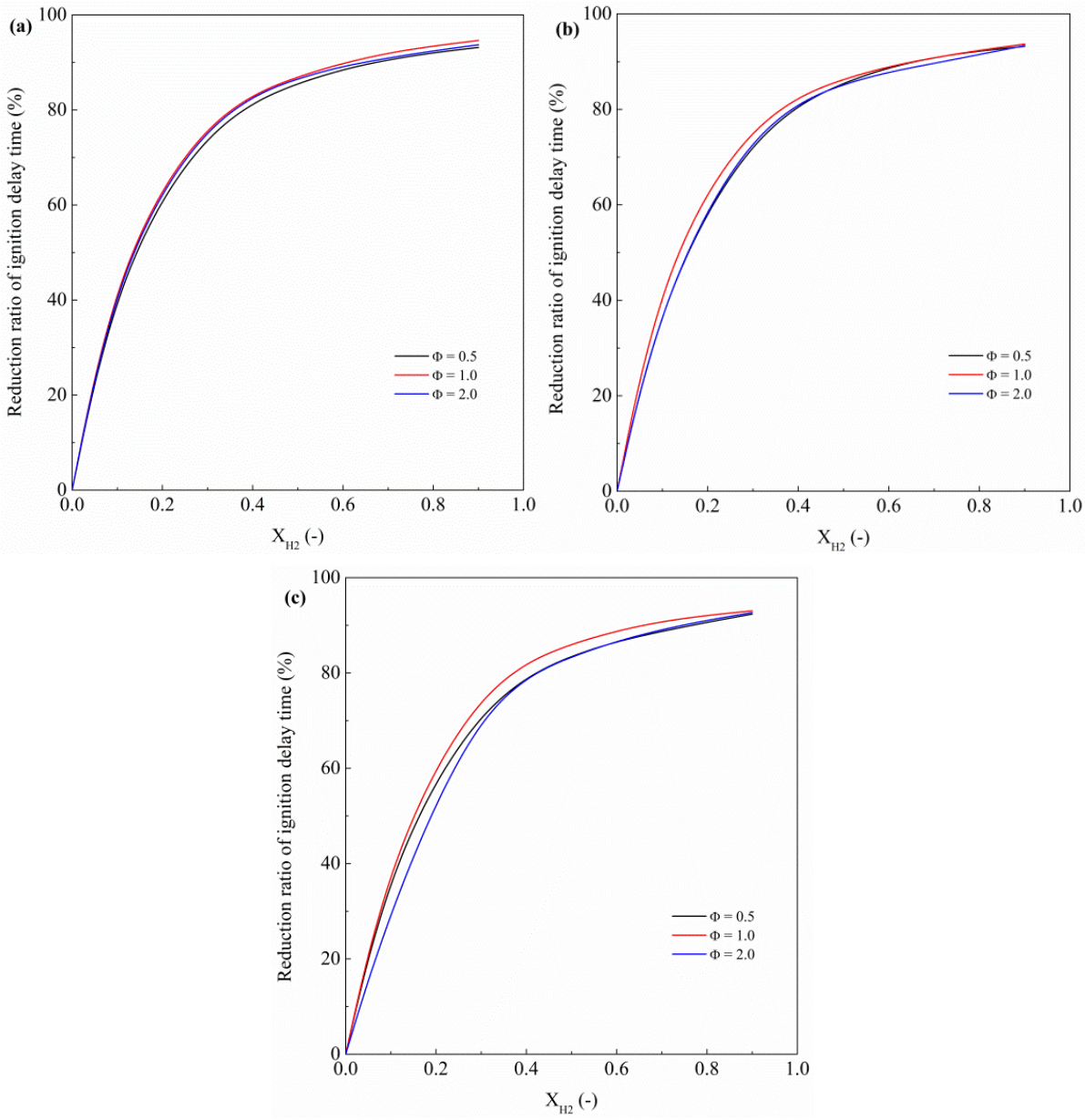

Fig. 13 Equivalence ratio effect on the reduction ratio of ignition delay time compared to pure NH_3 with various H_2 addition ratios over pressure of 1.4-30 atm at 1950 K: (a) P = 1.4 atm, (b) P = 11 atm, (c) P = 30 atm.

(a) ϕ = 0.5 and P = 1.4 atm (b) ϕ = 0.5 and P = 11 atm (c) ϕ = 0.5 and P = 30 atm

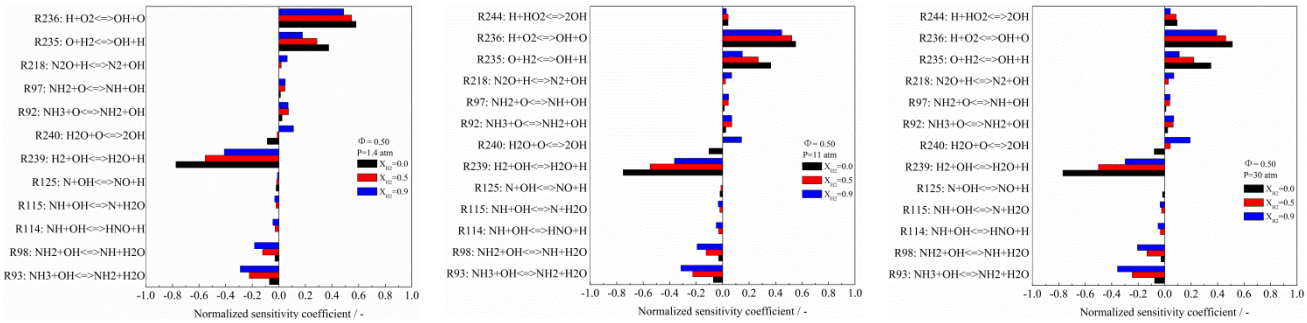

(d) ϕ = 1.0 and P = 1.4 atm (e) ϕ = 1.0 and P = 11 atm (f) ϕ = 1.0 and P = 30 atm

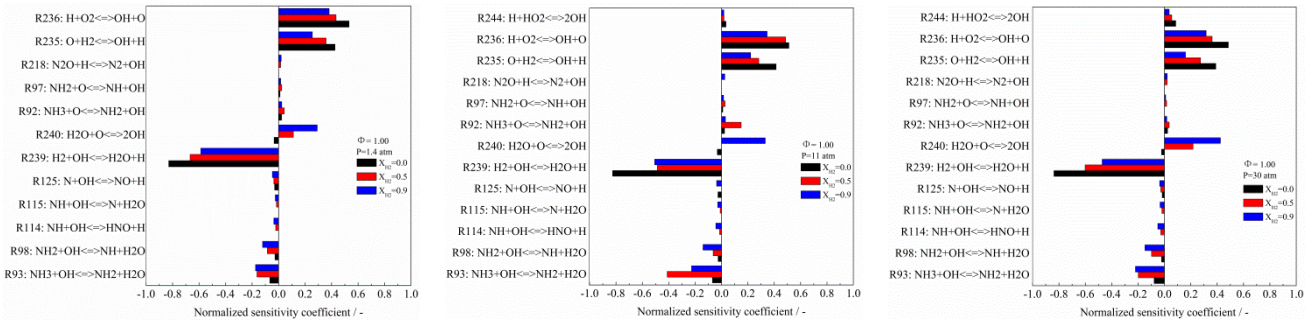

(g) ϕ = 2.0 and P = 1.4 atm (h) ϕ = 2.0 and P = 11 atm (i) ϕ = 2.0 and P = 30 atm

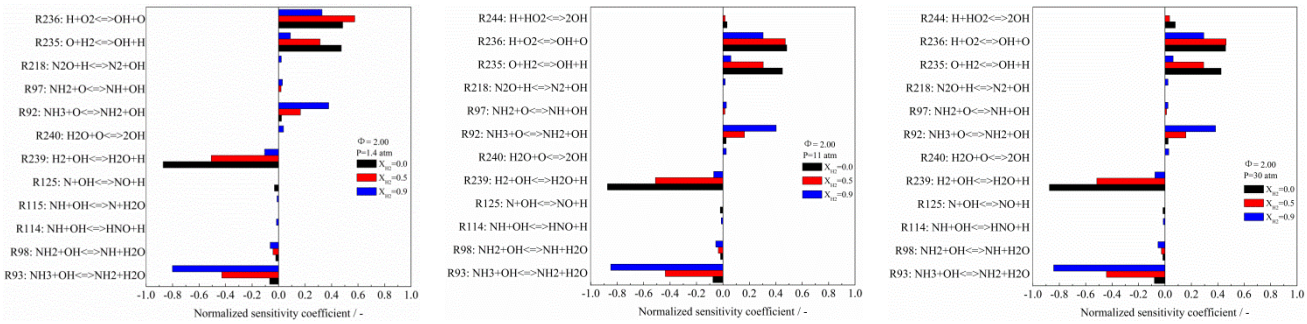

Fig. 14 Normalized sensitivity analysis of OH under DK mechanism with H_2 addition ratio of 0.0, 0.5, and 0.9 and ϕ of 0.5: (a) P = 1.4 atm, (b) P = 11 atm, (c) P = 30 atm; ϕ of 1.0: (d) P = 1.4 atm, (e) P = 11 atm, (f) P = 30 atm; and ϕ of 2.0: (g) P = 1.4 atm, (h) P = 11 atm, (i) P = 30 atm.

Appendix files:

Appendix A.rar

Appendix B.rar

Appendix C.rar